Eur. Phys. J. Plus (2018) **133**: 372
DOI 10.1140/epjp/i2018-12236-2

THE EUROPEAN PHYSICAL JOURNAL PLUS

Review

Comments on stellar evolution*

Mounib F. El Eid[a]

American University of Beirut, Department of Physics, Beirut, Lebanon

Received: 10 April 2018
Published online: 19 September 2018

Abstract. Given the limited space in this contribution, it is not possible to go into the details of the exciting astrophysical topic of stellar evolution and nucleosynthesis. It is attempted to emphasize the basics of this basic concept of the hydrostatic evolution of stars as they are driven by the interplay between gravity and nuclear energy generation, which is expressed by the virial theorem. In the case of massive stars roughly above $8\,M_\odot$, the breakdown of the hydrostatic evolution, due to the lack of nuclear energy generation, leads to gravitational collapse followed either by a successful supernova explosion, leaving a neutron star behind, or by a black hole, which is the ultimate end stage. The stars of masses in the lower mass range end their evolution as white dwarfs. The nucleosynthesis process in stars is a complex task. Most of the elements and their isotopes, especially the heavy elements, are produced in an explosive environment, or in the late stages of the asymptotic giant branch stars. The present paper will concentrate mainly on the evolutionary aspects, due to the to limited space given here.

1 Introduction

Stars are physical systems in which the four natural forces are coordinated. Their formation and evolution are complex, but they are described by fundamental physical laws. This is evidence that physical laws are universal. The existence of stars may reveal how human beings may consider themselves connected to the cosmos, simply because the elements in our bodies are synthesized in stars of many generations. Think about the DNA based on the carbon and nitrogen made in stars, and the hydrogen produced in the early Universe. Stars are always in interaction with their surroundings through their radiation, mass loss and ejection of enriched matter by supernova explosion, neutron star mergers, or though planetary nebulae formation. The understanding of star formation and evolution is only possible by comparing theoretical descriptions with observations, and this was made possible after the development of digital computers, which became faster in the course of time. The understanding of the internal structure of stars is accomplished by applying the basic stellar structure equation, which is briefly discussed in this paper. Before doing that, it is useful to show the basic characteristics of stars in a Hertzsprung-Russell diagram (HRD) (see fig. 1). This figure shows that:

i) Stars are divided into four groups: main sequence (MS), red giants (RG), supergiants (SG) and white dwarfs (WD). This division is fundamental and is linked to the evolutionary status of the stars.
ii) The masses increase along the MS, while the lifetimes decrease, meaning that the higher the mass the shorter the lifetime, since the luminosity (L) (or power) increases significantly with mass, like $L \propto M^{3.5}$ on the MS, where L is in solar units.
iii) The WDs are end evolutionary stages of low and intermediate-mass stars (IMS) in the mass range $(1–8)\,M_\odot$, which evolve beyond the RG stage through the asymptotic giant branch (AGB) stage, where they suffer thermal pulsations leading finally to heavy mass loss to become WDs. Higher masses cannot be shown in the HRD, because they undergo supernovae explosions and end up either as neutron stars or black holes. There is a clear relation between the spectral types of the star and its effective temperature (blackbody temperature). The spectral classification represents a temperature sequence, O-stars are hot and blue, while M-star are cool and red. Only with the help of the knowledge in modern physics, astronomer were able to understand the basis of these characteristics of stars.

* Focus Point on "Modern Astronomy: Selected Issues in Nuclear and High Energy Astrophysics" edited by S. Palmerini, O. Trippella.

[a] e-mail: meid@aub.edu.lb

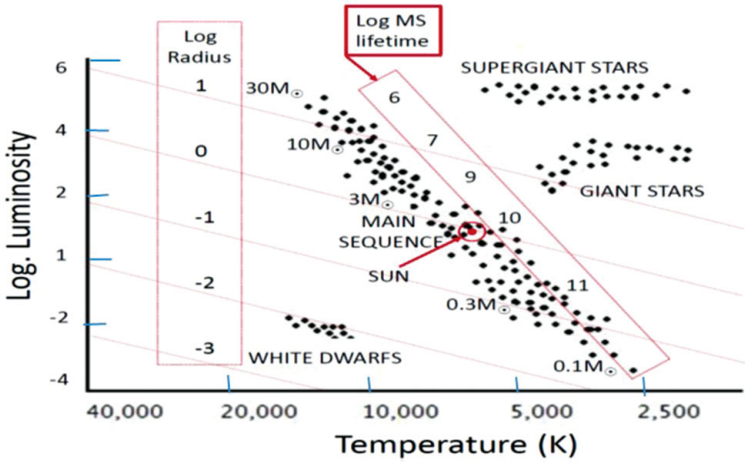

Fig. 1. Theoretical Hertzsprung Russell diagram showing how stars are divided into groups with their characteristics, see text.

It is interesting to consider the evolution of stars in the central temperature-density plane (T_c-ρ_c) as shown in fig. 2. Several comments can be made based on this figure.

a) The low-mass stars (LMS) and intermediate-mass stars (IMS) in the mass range (1–8) $M_\odot$ are the progenitor of the WDs as mentioned above. A subgroup in this mass range consists of stars up to masses of about 2.2 $M_\odot$, which evolve through the remarkable phase of the *He-flash* as seen in fig. 2(a). These stars are called (LMS). The helium-flash is a secular instability leading to thermal runaway. The reason for this is that each contraction brings the inner region of the star closer to the condition of electron degeneracy. After core hydrogen burning, the LMS stars develop cores in which the electron are degenerate due to he high density. Consequently, there is a common evolution of the central values indicated in fig. 2, implying that the cores have similar masses and their structure is nearly independent of the details of the star's envelope. This is a remarkable effect of the electron degeneracy achieved in these cores. The formation of a degenerate core does not imply that the star has reached the end stage of its evolution. This is because the hydrogen shell source continues to increase the mass of the core to a certain limit where the next burning phase occurs but now under degenerate conditions. This marks the onset of the *helium flash* in the LMS when the core mass exceeds about 0.45 $M_\odot$. The results shown in fig. 2(a) were discussed in [1]. Later calculation can be found in [2]. It is emphasized that despite of its violence, the helium flash does not disrupt the star, because the enormous energy released is absorbed by the expansion of the layers above the core. Observationally this is indicated by the existence of the well known *horizontal branch stars.*

b) The IMS which avoid the phase of He-flash, develop degenerate C-O cores of masses up to about 1.08 $M_\odot$ (see [3] for a review). The central evolution of these cores after He-burning occurs (see the trajectory of a 7 $M_\odot$ star in fig. 2(a), in a region where the neutrino energy losses become efficient to cool the inner core (see recent calculations in [4]). Their further evolution is characterized by a possible bifurcation either to the WD stage, or toward the phase of a *carbon flash.* The branching depends on whether the core mass $M_{\rm core}$ can increase to reach the so called *Chandrasekhar limit*, $M_{\rm ch} = 1.3\,M_\odot$ or higher (see [3]). An essential point here is that the envelope mass of the star should be massive enough, so that the core can grow by shell burning to reach $M_{\rm ch}$. The other possibility is that in a binary system the evolved star may accrete enough mass for its core to reach $M_{\rm ch}$. The outcome would be representing carbon flash as canonical model for type Ia supernovae. This discussion shows that a basic feature of the late evolution of IMS ($M \approx$ (2.2–8) $M_\odot$) is the competition between the decrease of the star's mass by mass loss and the increase of the degenerate C-O core toward the Chandrasekhar limit.

c) Stars with masses 13 $M_\odot$ and above can be considered as typical massive stars. After core carbon burning they ignite central neon-burning followed by oxygen and silicon-burning phases (see trajectory of a 25 $M_\odot$ star in fig. 2(b). After silicon-burning, these stars form cores of masses close to the Chandrasekehar limit consisting of iron-group nuclei. The ensuing evolution is characterized by the gravitational collapse of the iron core, where thermonuclear reactions are no more possible. At the onset of the collapse the central temperature and density are $T_c = 10^{10}$ K and $\rho_c = 10^{10}\,{\rm gcm}^{-3}$. If the collapse phase leads to a successful type-II supernova, then a neutron star will be formed, otherwise a stellar-mass black hole will be the ultimate fate.

d) Another region in fig. 2(b) is that of pair creation instability. Very massive stars in a mass range of excess of roughly 140 $M_\odot$ can evolve into such a region. A generation of such stars is distinct and termed *pop III stars.* They may have been formed (see [5]) as precalactic stars. It took relatively long time for the first stars to form in the universe. This may have occurred after the end of the *dark age*, or about 400 million years after the

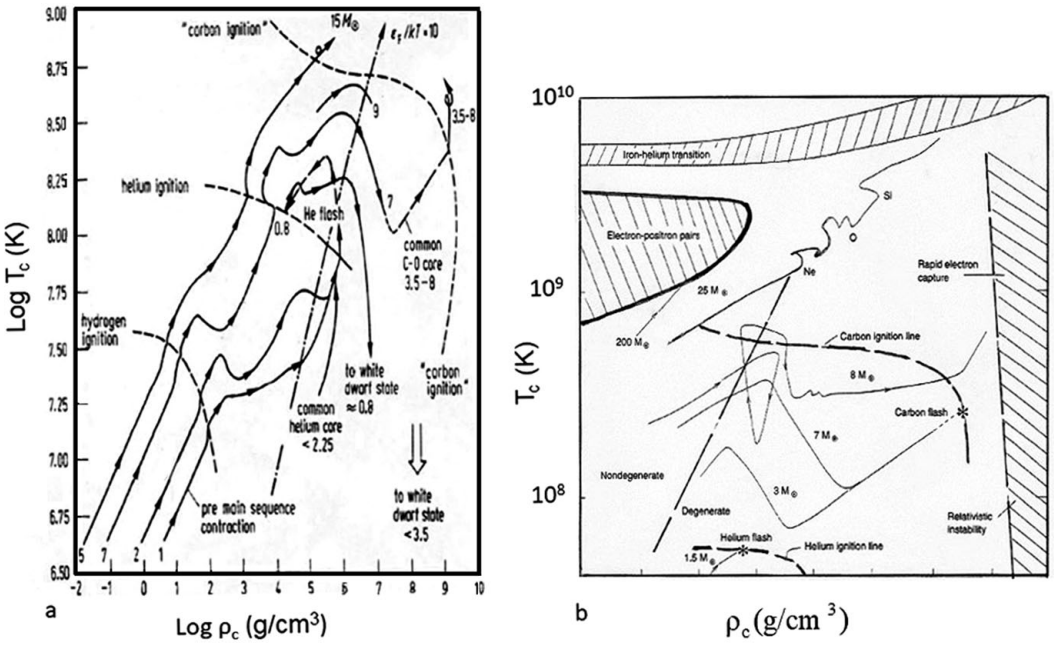

Fig. 2. Evolution of the central temperature T_c (in K) and central density ρ_c in (cm^{-3}) of the stars with the indicated masses in solar units. Ignition lines of relevant burning phases are defined by equating the neutrino losses to the nuclear energy generation rate. The dash-dotted lines divide the nondegenerate region from the degenerate region characterized by the degeneracy parameter $\varepsilon_f = \mu/\mathrm{kT}$. See text for details.

recombination epoch (about 380000 years after the Big Bang). These stars were likely very massive owing to the absence of heavy elements in the early molecular clouds where effective cooling and fragmentation were inhibited (see [5]). The basic mechanism of this instability is (see [6–8]) that the very massive stars develop massive C/O cores, which evolve toward the region of $e^- e^+$ pair creation by the intense radiation field (see fig. 2(b). The creation of the new particles decreases the radiation pressure, while the new particles do not add immediately their contribution to the pressure. At high density the adiabatic index Γ exceeds 4/3, because the electrons become degenerate, while at high temperatures the electrons and positrons become relativistic, so that the energy gap for the pair creations becomes unimportant. The net effect is that a bounded region in which Γ drops below 4/3. The collapsing core undergo explosive oxygen burning leading to a brilliant pair creation supernova (PCSN) releasing about 10^{52} erg.

A new insight concerning these peculiar events came through the observation and SN2007bi in a low metallicity dwarf galaxy about 1% the size of the milky way (see [9] for details), which seems to be a PCSN. One implications of such a discovery is that very massive stars are formed in the local universe in dwarf galaxies.

2 Summary of stellar structure equations

The results described above can only be understood by calculating the stellar structure and evolution with the aids of the stellar structure equations. The equations described below are written in spherical symmetry using Lagrangian coordinates, where the independent coordinates are the mass inside the radius r (M_r) and the time (t). The dependent variables are the velocity (u), pressure (p), temperature (T), density (ρ), and luminosity (L).

2.1 Momentum equation (gravitational interaction)

The momentum equation can be written (see [10]) as

$$\frac{\partial u}{\partial t} = -4\pi r^2 \frac{\partial p}{\partial M_r} - \frac{GM_r}{r^2}\,. \tag{1}$$

If the acceleration on the left-hand side of this equation is zero, then one deals with hydrostatic equilibrium, where the pressure gradient balances gravity. If the pressure gradient is zero, then one can derive a free fall time scale, which

can obtained as (see [10])

$$\tau_{ff} = 1.6 \times 10^3 \left(\frac{M}{\mathrm{M}_\odot}\right)^{-1/2} \left(\frac{R}{\mathrm{R}_\odot}\right)^{3/2} \mathrm{s}. \tag{2}$$

To appreciate this equation, $\tau_{ff} = 27\,\mathrm{min}$ for the Sun, but about 4.5 s for a white dwarf of a mass $1.0\,\mathrm{M}_\odot$ and a radius $0.02\,\mathrm{R}_\odot$. Thus, with this time scale no star can evolve to achieve hydrostatic equilibrium.

2.2 Velocity equation

$$\frac{\partial r}{\partial t} = u. \tag{3}$$

This equation describes the distribution of the velocity in the stellar model.

2.3 Mass conservation

$$\frac{\partial r}{\partial M_r} = \frac{1}{4\pi r^2 \rho}\,. \tag{4}$$

This equation is a form of continuity equation, if it is integrated over dr, it gives the mass with a radius r from the center.

2.4 Energy equation (strong, weak and electromagnetic interactions)

$$\frac{\partial L}{\partial M_r} = (\varepsilon_{\mathrm{nuc}} - \varepsilon_\nu) + \frac{p}{\rho^2}\frac{\partial \rho}{\partial t} - \frac{\partial \varepsilon}{\partial t}\,. \tag{5}$$

This equation is an expression of the energy conservation controlling the change of the luminosity distribution across the stellar model as determined by energy transport (usually radiative or convective), by the nuclear energy generation ($\varepsilon_{\mathrm{nuc}}$) in [erg/g · s] due to the thermonuclear reactions occurring in the interior of the star, and by the energy losses due to diverse neutrino processes which become effective after the core-helium-burning phase (see text by [10]) and stream out of the star. The third and forth terms in eq. (5) represent the work due to contraction or expansion and the rate of change with time of the internal energy. These two term describes the gravitational energy term (ε_g being positive in case of contraction or negative in case of expansion). Note that these two terms balance each other in the case the thermal equilibrium.

Since a star must emit radiation an equation of energy transport must be added to the above equations (see eq. (7)). One can estimate the so-called *Kelvin-Helmholtz time scale* (τ_{KH}), which characterizes the relaxation time needed for a star to return to thermal equilibrium. By simply comparing (see [10]) the average potential energy of the star to the luminosity, one finds

$$\tau_{\mathrm{KH}} \approx 2 \times 10^7 \left(\frac{M}{\mathrm{M}_\odot}\right) \text{ years}. \tag{6}$$

Applying this time scale to the Sun gives $\tau_{\mathrm{KH}} = 2 \times 10^7$ years, which is extremely shorter than the lifetime of the Sun. We will see this below when the nuclear time scale is introduced. Since a star must emit radiation an equation of energy transport must be added to the above equations.

2.5 Energy transport equation

$$\frac{\partial T}{\partial M_r} = -\frac{GM_r T}{4\pi r^4 P}\nabla. \tag{7}$$

In this equation $\nabla \equiv \frac{\mathrm{d}\ln T}{\mathrm{d}\ln p}$ is either the radiative gradient or the convective gradient depending on the characteristic of the stellar layer. If the interior stellar layer is radiative, then radiative energy transfer is described as a diffusion process, and the temperature gradient in eq. (7) is given by

$$\nabla \equiv \nabla_{\mathrm{rad}} = \frac{3}{16ac\pi G M_r}\frac{\kappa L_r P}{T^4}\,. \tag{8}$$

In this equation, κ is the *Rosselland mean opacities*, which can be obtained from the extended calculations in [11].

In the case of a convective stellar layer, the determination of the temperature gradient is more complex than in case of radiative transfer. Convective instability in local approximation is determined according to the *Schwarzschild criterion* for convective instability, which is a dynamical instability meaning that a convective mass element moves essentially adiabatically between two layers. This is expressed mathematically (see [10] for details) as $\nabla_{\mathrm{rad}} < \nabla_{ad}$

for stability against convection, where $\nabla_{\rm rad}$ is given in eq. (8). The adiabatic temperature gradient is defined as $\nabla_{ad} \equiv (\frac{\partial \ln T}{\partial \ln p})_s$, taken at constant entropy, since for adiabatic change the entropy remains constant. Then using the first law of thermodynamics with $\mathrm{d}s = 0$, yields $\nabla_{ad} = \frac{P\delta}{T\rho c_P}$, where $\delta \equiv -(\frac{\partial \ln \rho}{\partial \ln T})_p$, a quantity that can be determined by a given equation of state $P = P(\rho, T)$. The temperature gradient is close to the adiabatic gradient only in the deep inferior of the star. The atmospheric layers are superadiabatic. The common way used in stellar evolution is to use the *mixing length theory* (MLT) to obtain the temperature gradient. A complete discussion of this approach is given in the text by [10].

A difficult problem arises in the treatment of convection in the context of the local approximation. This concerns the determination of the border of a convective region according to the *Schwarzschild criterion*. Convective elements may overshoot the boundary as determined by this criterion. Several works deal with this issue [12–14]. The essential point is that overshooting depends on the convective velocity, which is proportional to $(\nabla_{\rm rad} - \nabla_{ad})$ and can be obtained from the MLT (see [10]). At the boundary, this difference approaches zero but convective elements may still penetrate into the radiative zone leading to extra mixing without influencing the energy transport. This extra mixing will not be complete, because acting against buoyancy and viscosity, rather it would be exponentially decaying. In the treatment by [13], mixing is accomplished by solving a diffusion equation, where a diffusion coefficient is adopted as suggested by hydrodynamical calculations according to [15] and is given as

$$D = D_0 \exp\left(-\frac{\delta r}{\beta H_p}\right). \tag{9}$$

Here, D_0 is the diffusion coefficient at the boundary as determined by the Schwarzschild criterion, $\delta r = r - r_0$ the distance from this boundary extended in terms of the pressure scale height (H_p) with β being a free parameter which determines the efficiency of the extra mixing into the radiative layers. Unfortunately, there is no general way to fix this parameter and it is not the same for different convective-radiative borders. To get a feeling for its value, we quote the value $\beta \sim 0.1$ used by [12] to obtain a maximum extension of the ^{13}C-profile (or pocket) in thermaly pulsating AGB stars.

2.6 Nuclear transmutation

The thermonuclear reactions occurring in stellar interiors are responsible for the evolution of stars and they essentially determine their lifetimes. The change of nuclear species may be described as follows:

$$\frac{\mathrm{d}Y_i}{\mathrm{d}t} = \sum_j N_j^i \lambda_j Y_j + \sum_{j,k} N_{j,k}^i \rho N_A \langle \sigma v \rangle_{j,k} Y_j Y_k + \sum_{j,k,l} N_{j,k}^i \rho^2 N_A^2 \langle \sigma v \rangle_{j,k,l} Y_j Y_k Y_l. \tag{10}$$

In this equation, the abundance is denoted by $Y_i = \frac{X_i}{A_i}$ (mass fraction over mass number), where $N_j^i = N_i$, when the process of weak interaction or that of photodisintegrations are involved. However, $N_{j,k}^i = N_i/(N_j!N_k!)$ for two-body reactions, and $N_{j,k,l}^i = N_i/(N_j!N_k!N_l!)$ for three-body reactions. The fractorials are required to avoid double counting in the case of identical poarticles, such as the $p+p$ reaction or the triple-alpha reaction. Note that λ_j in the above equation represents the rate of weak interaction or photodisintegration, while the terms $N_A\langle \sigma v \rangle$ is a Maxwellian average cross sections.

The nuclear time scale can be obtained by $\tau_{\rm nuc} = \frac{\Delta m c^2}{L}$, that is the change of mass divided by the luminosity of the star. For example, during hydrogen burning by the proton-proton chain in stars of masses $\leq 1.5\,\mathrm{M}_\odot$ or by the CNO cycle in higher masses, $4\,^1\mathrm{H} \rightarrow {}^4\mathrm{He}$ is the net outcome of this burning phase. Then one finds (see [10]) that

$$\tau_{\rm nuc} < 1.05 \times 10^{11} \left(\frac{M}{\mathrm{M}_\odot}\right) \left(\frac{L}{L_\odot}\right)^{-1} \text{ years}. \tag{11}$$

Applying this equation to the Sun, we get 10^{11} years, which is too high, so that about only about $0.1\,\mathrm{M}_\odot$ is involved to match the main sequence age of about 10^{10} years. Comparing all the three time scales we have discussed, the learn effect is that

$$\tau_{ff} \ll \tau_{\rm KH} \ll \tau_{\rm nuc}. \tag{12}$$

We will demonstrate this crucial inequality in sect. 4.

3 Solving the stellar structure equations

It is beyond the scope of the present contribution to describe the numerical methods used to solve the above set of partial differential equations. The basic problem is a combination of an initial value problem with a boundary-value problem. At each time step, the structure of the star is obtained by matching given boundary conditions. Since there are five equations as outlined above, five boundary conditions are needed, three at the center ($r = 0$, $L = 0$, $u = 0$) and two surface boundaries. To define the surface is not easy, because stars have extended atmospheres not in thermal equilibrium. A common way in stellar evolution is to adopt a blackbody surface with an effective temperature according the Stefan-Boltzman law, $L = 4\pi R^2 \sigma T_{\rm eff}^4$. Still, an effective density is to be used at the boundary. The so-called gray atmosphere (or Eddington approximation) may be used, where an effective density can be obtained from $T^4 = \frac{3}{4}(\tau + 2/3)$ (see [16]) with the ideal gas equation of state. The effective density can be obtained (see [17]) as

$$\varrho_{\rm eff} = \frac{2\mu}{3\kappa\Re T_{\rm eff}} \frac{GM}{R^2} \left(\frac{L_E - L}{L_E} \right), \tag{13}$$

where $L_E = 4\pi cGM/\kappa$ is the Eddinton luminosity, κ is the Rosseland mean opacity, and μ is the mean molecular weight. Having assigned the boundary conditions, the equations are transformed into difference equations, using a variable grid connecting shells $(i-1, i, i+1,\ i = 1, N)$, where the flux quantity like r, u and L are centered at the grid, others are averaged between the grids. Newton-Raphson Iteration is executed to find the roots of the five equations. This method is a hydrodynamical scheme implemented by the author and his collaborator when he was at the observatory of the University of Göttingen/Germany till 1994. This code has received some modifications (see [18] for details).

4 Stellar evolution

It is not possible to cover the many aspects of stellar evolution in the limited space of the present paper. Examples are chosen to illustrate some main characteristics of the evolution.

4.1 Comments on the evolution of low and intermediate mass stars

It is Interesting to describe the evolution of low and intermediate stars. The evolution of a $5\,M_\odot$ star in the Hertzsprung-Russell diagram (HRD) is shown in fig. 3. Details of this evolution are as follows.

- Starting at the zero-age main sequence (marked 1), the $5\,M_\odot$ star evolves through core-H-burning between the positions 1 to 3, transforming hydrogen mainly into ^{4}He and some ^{14}N by the CNO cycle. This occurs in a convective core (see right panel of fig. 3). The star evolves on the nuclear time scale $\tau_{\rm nuc}$ described above, which is absolutely the longest due to the largest energy release by H-burning.
- After the end of core-H-burning, the star has no nuclear energy source left. Consequently, gravity takes over leading to its overall contraction, so that the H-rich layer surrounding the hydrogen-free core (called He-core) achieves the temperature for the CNO-cycle to be effective. This occurs nearly at position 4. This Shell H-burning inflates the star, which evolves toward the red giant branch (RGB) beginning at the position 5. During the expansion of the star's outer layers, the opacity increases and leads to the formation of a deep convective envelope (see right panel), which extends to the stellar layers that were processed by the H-burning and this called first dredge up (FDUP), *i.e.* mixing to the surface of mainly ^{4}He and ^{14}N. The position 5 marks the ignition of core He-burning, which proceeds again in a convective core, but now increasing in mass due to the increasing opacity, because lighter materials lie above heavier ones. Increasing opacity promotes convective instability, so that the convective envelope is formed between the points 5 to 7 indicating the RGB.
- As the star ascends the RGB, its core keeps contracting until the central temperature of 10^8 K is reached needed for He-ignition. Core-He-burning contributes thereafter to the nuclear energy generation rate diminishing the contribution of the H-burning shell and this leads the luminosity to decrease as seen after point 7. The ensuing evolution of this star is characterized by the formation of a *blue loop* (between positions 8 and 9). The star returns to the RGB to complete the last phase of the core-He-burning (position 10). This leads the inner core being devoted of He to contact seeking the next nuclear fuel which will be the core carbon burning. While this happen the shell H-burning leads to the expansion of the outer layer thus to the raising luminosity and causing the envelope to become convective again penetrating deep enough to lead to a second dredge up (SDUP) mixing up to the surface elements like ^{4}He, ^{12}C and ^{14}N. This SDUP is rather sensitive to the efficiency of the H-shell source which acts as entropy barrier in stars of $M \leq 4\,M_\odot$ preventing the deep penetration to enable the SDUP.

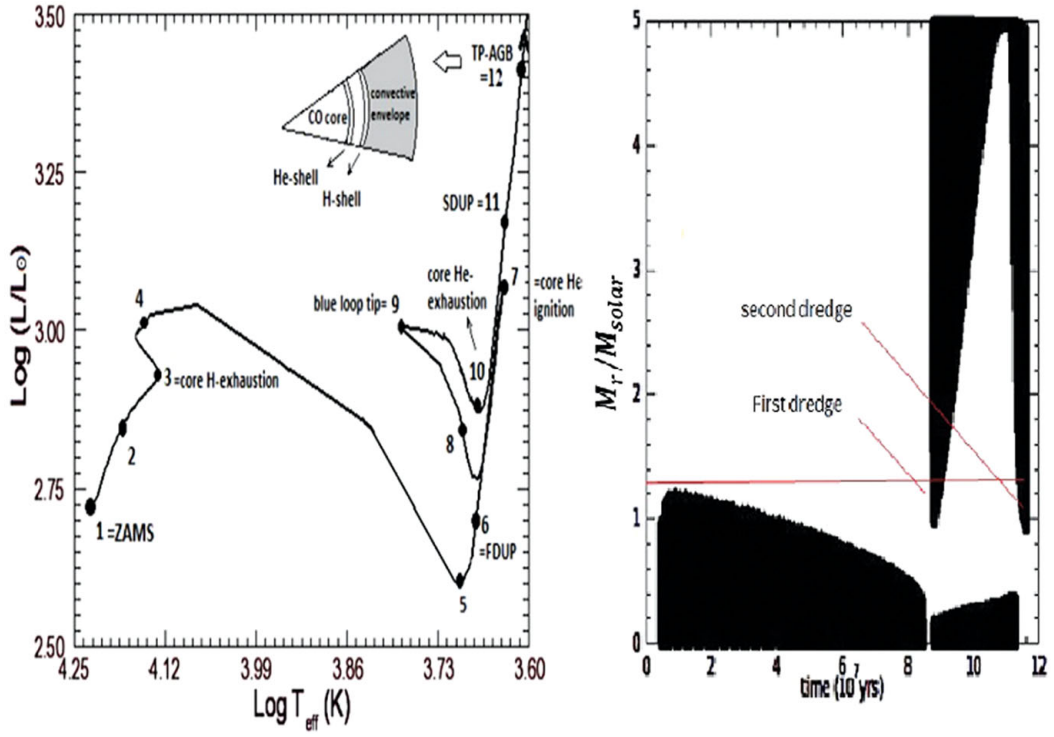

Fig. 3. Evolution in the HR diagram (left) and structure evolution of a $5\,M_\odot$ star of initial solar-like initial composition. (Right) Dark areas are convective regions, others are radiative regions; see text for explanation.

– After position 10 in fig. 3, the star reaches the stage of asymptotic giant branch AGB. This stage initiate the phase of thermal pulsating after which the stars end up as *white dwarfs*. The structure of an AGB stars is shown in the inset of fig. 3 with a core mainly composed C and O surrounded by a He-rich shell, a buffer zone and a H-rich shell. A large body of works deals with the thermally pulsations on the AGB. It is a very interesting evolutionary phase of LMS and IMS stars for many reasons. They are the progenitors of white dwarfs, the site of the s-process nuclosynthesis that produces about half of the heavy elements and their isotopes beyond copper, and they constitute a challenging task of stellar modelling concerning thermal pulsation. Review articles on AGB stars and their thermal pulsation leading to the so called third dredge up (TDUP) are given by [19,20] and references therein. We also mention an interesting review on heavy elements in the early galaxy by [21]. The challenging problem in the simulation of the TDUP is to follow the penetration of the convective envelope between two pulses into the He/C region after the power down of the He-flash. The longstanding problem is how to describe correctly the diffusion of protons into the carbon-rich layers in order to create the right amount of ^{13}C via the $^{12}C(p,\gamma)^{13}N(\beta^+,\nu)^{13}C$ in order to understand the neutron source for the main component od the s-process created via the reaction $^{13}C(\alpha,n)^{16}O$. The hydrogen ingestion into He-burning zone in super AGB stars (7–10) $M_\odot$ has been studied by [22].
– What are the reasons behind the formation of such a loop which are formed by all stars in the mass range (4–12) $M_\odot$? Figure 4 shows tracks with their loops which lie in the range where the δ-cepheids variable are found. We briefly describe the physical background of these loops here and refer to more detailed discussion in [10, 23, 24]. Various aspects of stellar evolution are involved in the formation of these loops. They may be summarized as follows.
– A major effect on the formation of the blue loops is the efficiency of shell H-burning. A key role plays the reaction rate of $^{14}N(p,\gamma)^{15}O$ which controls the energy generation rate of the CNO cycle operating in the shell-H-burning in IMS. This is illustrated in fig. 4, where the tracks shown in the right panel are obtained with a lower ^{14}N-rate leading to remarkable suppression of the loop extension in the mass range (5–7) $M_\odot$. Details about these calculations are given in [23]. One sees that the behavior of the loops is sensitive to the star's mass as well.
– Another point has been already mentioned in the text by [10] is that the efficiency of the H-shell source depends on how the hydrogen profile is processed. Clearly, envelope convective mixing plays important role in determining the H-profile. This is illustrated with the help of fig. 5 (see details by [23]), which shows the evolution of a $6\,M_\odot$ star during core helium-burning and loop formation. Note that the whole evolutionary track of this star is shown in fig. 4. The interpretation of this figure is as follows.

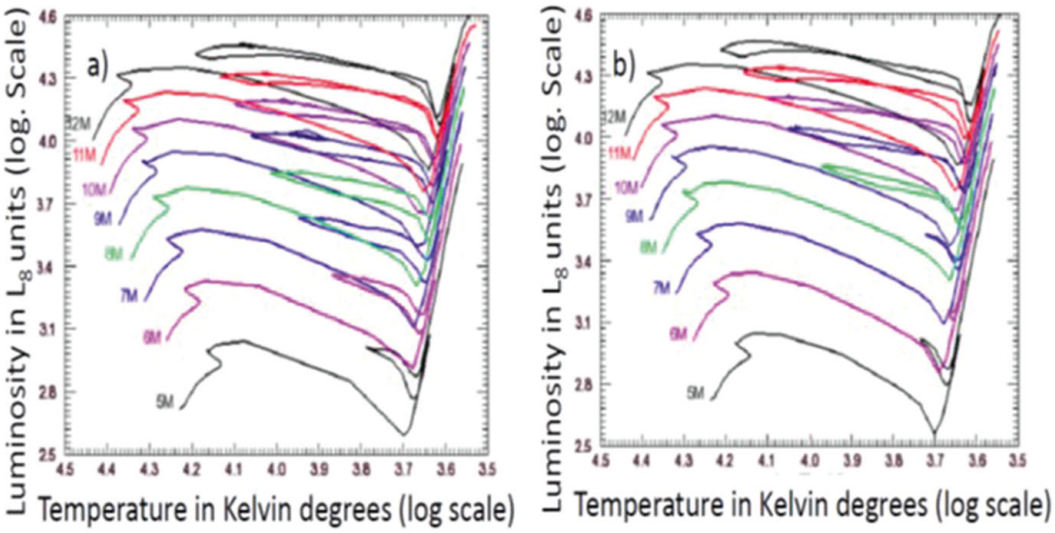

Fig. 4. Evolutionary tracks of intermediate-mass stars of solar-like intimal composition. The only difference between the tracks in the left panel and those in the right panel is using different rate for the reaction $^{14}\mathrm{N}(p,\gamma)^{15}\mathrm{O}$ controlling the energy generation rate in the CNO cycle. Note that the lower rate used to obtain the tracks in the right panel led to remarkable reduction of the loop extension in the mass range (5–7) $\mathrm{M}_\odot$, see text.

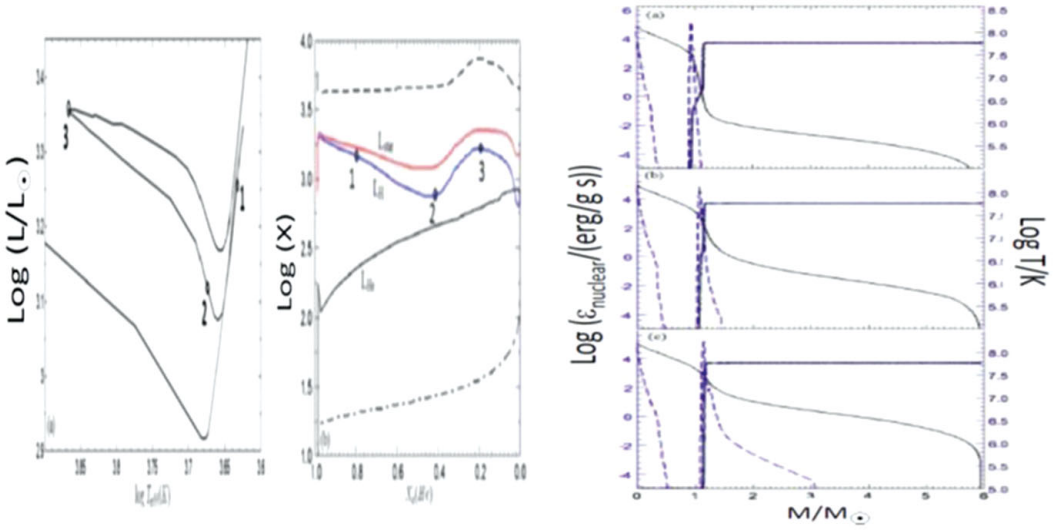

Fig. 5. Evolution of a 6 $\mathrm{M}_\odot$ star described showing snapshots of the hydrogen profile and the energy generation rates due to shall-H-burning together with the central He-burning. These figures illustrate what happens during the blue loop formation, see text for details.

The evolution during the stages 1 to 3 in the left panel correspond to those in the adjacent figure, showing the variation of the luminosity, L_{star}, L_{H}, and L_{He}, which are integrated quantities. It is seen that L_{H} supplies the major part of the star's luminosity, except toward the late phase of core He-burning after (point 3). However, L_{H} decreases gradually between points 1 and 2, because the H-shell source has processed part of the H-profile as seen in the figure on the right, corresponding to the stages between 1 to 3. After position 2, a remarkable increase of the H-shell source is noticeable and this enforcing of the shell burning is due to the merging of the H-shell source with the H-profile (see snapshot at right bottom)). The enforced H-shell burning is concurrent with the loop formation. This discussion shows that the formation and extension of blue loops are rather sensitive to the efficiency of the shell H-burning, but in a subtle way, since this burning depends on the $^{14}\mathrm{N}(p,\gamma)$-rate and how deep the convective envelope penetrates into the layers of shell-H-burning. The treatment of the penetration of the convective envelope is essential as described in [23] and [25].

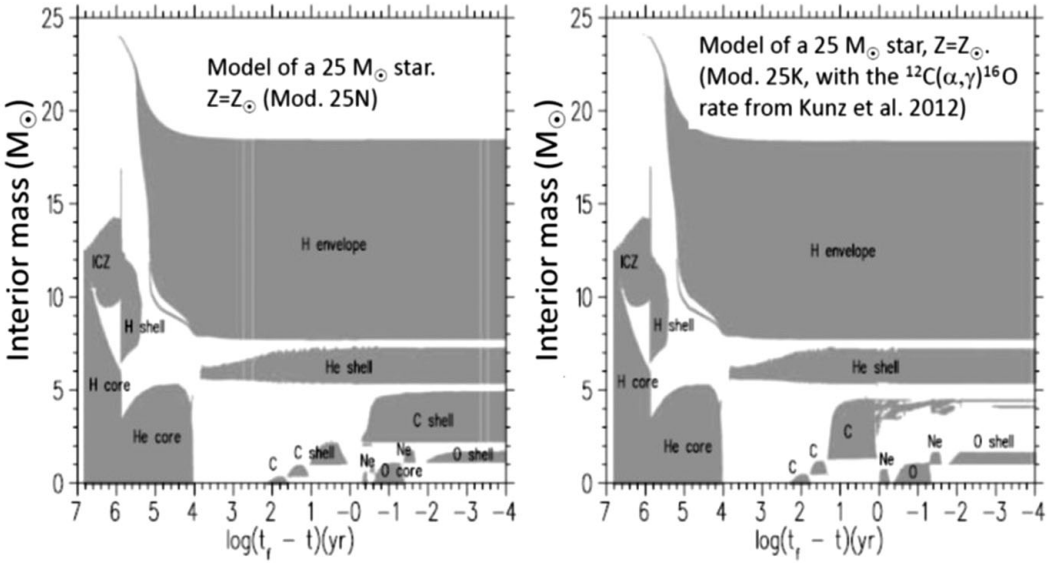

Fig. 6. Change of internal structure as a function of time of a $25\,M_\odot$ star of initial solar-like composition: the left panel is referred to as 25N, the right panel as is referred to as 25K. The stars are evolved from the main sequence till shell-oxygen burning. Dark areas represent convective regions. The x-axis is a logarithmic scale for the lifetime, where t_f is the time of the last calculated stellar model, see text.

4.2 Comments on the evolution of massive stars

The evolution of massive stars is another complex task in astrophysics. Their presupernova evolution is complicated as well as the description of their final stages which may lead to supernova explosion or black-hole formation. We pick up an interesting case focusing on the evolution of a massive star of $25\,M_\odot$ through the core carbon and shell-carbon-burning phase. We link this discussion to the role of the reaction $^{12}C(\alpha,\gamma)^{16}O$. A long review article was recently devoted to this relation, which is challenging from the nuclear physics point of view (see [26]). Here we illustrate the importance of this reaction in case of massive star evolution. Figure 6 shows the evolution of a $25\,M_\odot$ star of a solar-like initial composition. In this calculation according to [18] two different rates have been used. The results shown in the right panel of fig. 6 were obtained using the rate according to [27] (*sequence* 25K), the rates used to obtain the results shown in the lift panel are based on the rate presented by the NACRE collaboration [28] (*sequence* 25N). The NACRE rate is higher in the temperature range of core-He-burning (0.13–0.40) $\times\,10^9$ K. Interesting implications are found when comparing these two rates.

a) As a result of core He-burning, central carbon mass fraction is $X(^{12}C) = 0.24$ in 25K, but 0.28 in 25N. The lower value in 25N is due to the higher rate of $^{12}C(\alpha,\gamma)^{16}O$ in 25N which becomes effective during the late phase of core He-burning. The implication of this difference appears at the onset of core carbon burning, where in the case of 25K a convective core forms with a mass of $0.47\,M_\odot$, while in case 25N this mass is $0.36\,M_\odot$. The larger core mass in 25K is related to the different values of the carbon mass fraction resulting at the end of core He-burning. This is because a larger $X(^{12}C)$ leads to higher and positive effective energy generation rate $\epsilon_{\rm eff} = (\epsilon_{\rm nuc} - \epsilon_\nu)$ appearing in eq. (5). This result is along the finding by [29] for a $25\,M_\odot$ star, who have used two different rates for the $^{12}C(\alpha,\gamma)^{16}O$, one rate according to [30] and the other rate is according to [31]. In the temperature range of core-He-burning as mentioned above, the ratio CF85 rate was about factor of 2.7 larger than that of the rate CF88. Consequently, $X(^{12}C) = 0.18$ was obtained for the rate Cf85, but 0.42 with the smaller C88-rate. Furthermore, in case of the higher rate the calculation did not lead to a formation of a convective core at the onset of central-carbon-burning. In contrast, a convective core was formed with the lower rate.

b) The evolution through the central-C-burning has a strong effect on the ensuing phases, in particular, shell-C-burning is to be mentioned because it contributes to the weak component of the s-process nucleosynthesis (see [32] for a recent work). As seen in fig. 6, shell-C-burning exhibits different behavior depending one the characterises of the previous core burning phase, and proceeds in several episodes seen in the figures. The main reason for that is related to the shape od the carbon profile as it is formed at central carbon-burning. The conclusion of this discussion is that the late phases of massive stars are depending on the previous hydrogen- and helium-burning phases. Realizing that the s-process products are ejected in a supernova explosion only from the core He-burning and shell C-burning means that a careful treatment of these phases is indispensable.

5 Concluding remarks

To summarize the main stream of this contribution:

a) Stellar evolution and nucleosynthesis are exciting part of astrophysics. They illustrate that physical laws are universal. The stars in different generation created for us the elements carbon and beyond. We are made from that dust.
b) Calculating stellar structure and evolution is a challenging task, not only on numerical bases but also on physical grounds. The treatment of mixing is one main problem. Future work would eventually be a three dimensional modelling that helps to justify a local description of convective mixing. Effects of rotation and magnetic field cannot be ignored.
c) The formation of the elements and the isotopes, from carbon and beyond, is only possible in stars. In particular the formation of heavy elements beyond iron is astonishing and needs various sites. The s-process requires the thermal pulsations of the AGB stars and the core He-burning and shell C-burning. The site of the r-process was thought to be the supernova explosions of massive stars. New observations indicate the neutron star mergers seem to constitute an essential site of the r-process. A new paper is dealing with this new insight (see [33]).

The author thanks the organizer of the fourth Azarquiel school for supporting his trip and for their great work in offering that school. He thanks his colleague and friend M. Busso for his assistance in finishing this manuscript.

References

1. I. Iben Jr., A. Renzini, Phys. Rep. **105**, 329 (1984).
2. M.F. El Eid, Astron. Astrophys. **285**, 915 (1994).
3. K. Nomoto, M. Hashimoto, Phys. Rep. **163**, 13 (1988).
4. J. Jose, G. Hallabi, M.F. El Eid, Astron. Astrophys. **593**, A54 (2016).
5. V. Bromm *et al.*, Nature **459**, 49B (2009).
6. W.W. Ober, M.F. El Eid, K.J. Fricke, Astron. Astrophys. **119**, 61 (1983).
7. A. Heger, S.E. Woosley, Astrophys. J. **567**, 532 (2002).
8. V. Bromm *et al.*, Nature **459**, 29 (2009).
9. Gal-Yam *et al.*, Nature **462**, 579 (2009).
10. R. Kippenhahn, A. Wegert, *Stellar Structure and Evolution* (Springer Verlag, Berlin, 1990).
11. F.J. Roger, C.A. Iglesias, Astrophys. J. Suppl. **79**, 507 (1992).
12. O. Straniero *et al.*, ASP Conf. Ser. **497**, 259 (2015).
13. F. Herwig *et al.*, Astron. Astrophys. **324**, L81 (1997).
14. L. Deng, D.R. Xiong, Mon. Not. R. Astron. Soc. **386**, 1979 (2008).
15. B. Freytag *et al.*, Astron. Astrophys. **313**, 497 (1996).
16. B.W. Carroll, D.A. Ostile, *An Introduction to Modern Astrophysics* (Pearson, New York, 2007).
17. B. Paczynski, M. Rozyczka, Acta Astron. **25**, 213 (1977).
18. M.F. El Eid, L.-S. The, B.S. Meyer, Space Sci. Rev. **147**, 1 (2009).
19. F. Herwig, Annu. Rev. Astron. Astrophys. **43**, 435 (2005).
20. M. Busso *et al.*, Annu. Rev. Astron. Astrophys. **37**, 239 (1999).
21. C. Sneden, J.J. Cowan, R. Gallino, Annu. Rev. Astron. Astrophys. **46**, 241 (2008).
22. S. Jones *et al.*, Mon. Not. R. Astron. Soc. **455**, 3848 (2015).
23. G.M. Halabi, M.F. El Eid, A. Champgane, Astrophys. J. **761**, 10 (2012).
24. M. Salaris, S. Cassisi, *Evolituon of Stars and Stellar populations* (Wiley:Chichester West Sussex, UL, 2008).
25. A.-J. Lai, Y. Li, Res. Astron. Astophys. **11**, 1351 (2011).
26. R.J. de Boer *et al.*, arXiv:1709.03144v1 (2107).
27. M. Kunz *et al.*, Astrophys. J. **567**, 643 (2002).
28. M. Angulo *et al.*, Nucl. Phys. A **656**, 3 (1999).
29. G. Imbtriani *et al.*, Astrophys. J. **558**, 903 (2001).
30. G.R. Caughlan *et al.*, At. Data Nucl. Data Tables **32**, 197 (1985).
31. G.R. Caughlan *et al.*, At. Data Nucl. Data Tables **40**, 283 (1985).
32. L.-S. The, M.F. El Eid, B.S. Meyer, Astrophys. J. **655**, 1058 (2007).
33. F.K. Thielemann *et al.*, Annu. Rev. Nucl. Part. Sci. **67**, 253 (2017).